# OPTIMAL ROCK PROPERTY TRENDS IN NORMAL PRESSURE FORMATIONS IN AN OFFSHORE NIGER DELTA FIELD

L. O. Onuorah[1], K. K. Nwozor[2,3]

[1]Department of Physical and Geosciences, Godfrey Okoye University, Ugwu-omu Nike, Nigeria;[2]Department of Geology and Petroleum Geology, University of Aberdeen, Aberdeen, United Kingdom;[3]Department of Geology, Chukwuemeka Odumegwu-Ojukwu University, Uli, Nigeria;E-mail: lorettaonuorah@yahoo.com; kknwozor@yahoo.com

**Abstract**

Rocks as natural materials are inhomogeneous and anisotropic with the implication that their physical properties are never the same but rather vary in depth, time and space. A good understanding of rock parameters at deep and challenging settings helps improve the interpretation of essential exploration data. Vital to this improved knowledge is the need to establish a threshold of normal and standard rock property behaviours in target areas in order to detect abnormal trends that could be critical to exploration success. Analyses of rock property trends in a normally pressured reservoir in Offshore Niger Delta have been carried out using wireline log data such as sonic, density, resistivity and gamma ray logs. The petrophysical workflow involved the generation and interpretation of cross-plots of density – $V_p$, and Poisson's ratio - $V_p$; and depth trends of $V_p$, $V_s$, density, acoustic impedance and Poisson's ratio for sands and shales. A predictable linear relationship exist in these plots; it is normal for velocity, density and acoustic impedance trends to increase with depth due to progressive mechanical compaction while Poisson's ratio decreases with depth.

*Keywords:* normal compaction; rock property; crossplots; Offshore; Niger Delta.

## 1. Introduction

Rock property trends are vital to the understanding and predictability of subsurface environments. Good petrophysical and formation evaluation decisions are guided by accurate knowledge of wireline log responses as dictated by the subsisting geology. Calibrations from such evaluations equally provide the basis for the constraining and interpretation of pre-drill exploration data [13]. In order to understand the expected well log response on a siliciclastic reservoir, it is of key interest to know the trends and contrasts in elastic properties between shales and sands as a function of depth. Modeled depth trends help in the understanding of observed depth behaviour of rock properties and to detect anomalous intervals that could be critical to exploration, drilling and production success. These abnormal zones could be due to unusual formation pressure variations, changes in lithologies or abrupt diagenetic events.

In most sedimentary environments, it is normal for velocities and densities of siliciclastic sedimentary rocks to increase with depth. This trend is as a result of progressive mechanical compaction and its consequent porosity reduction [1,12]. Castagna *et al.* [6] reported on the relationship between P-wave and S-wave velocities in clastic silicates and revealed that to the first order, compressional velocity ($V_p$) in water-saturated clastic silicate rocks is almost linearly related to shear velocity ($V_s$) such that increasing compressional velocity leads to a decrease in the $V_p/V_s$ ratio. On the contrary, $V_p/V_s$ ratio is nearly constant in dry sandstones with the implication that rigidity tends to equal bulk modulus. These authors obtained a general equation relating $V_p$ to $V_s$, which they called the mud rock line equation. Cross-plots of Poisson's ratio and $V_p$ for water saturated rock indicates an approximate linear relationship, while Poisson's ratio of air saturated rocks is constant [6]. Bruce and Bowers [5] and Bowers [4]

used depth plots of sonic velocity, density, and resistivity to show the cross over from hydrostatic pressures to high formation pressures.

## 2. Description of Study Area

The study area lies in the Nigerian sector of the Atlantic Ocean in the oil-rich Niger Delta region (Figure 1). The Niger Delta sedimentary basin is a clastic environment dominated by sands and shales. Its history is associated with the rifting that led to the development of the Benue Trough. The delta is made up of three major lithostratigraphic formations namely the Akata, Agbada and Benin. The Akata Formation is a marine deposit that comprises mainly clays and is believed to be the source rock of hydrocarbons in the area. It is succeeded by the sandstones and clays of the hydrocarbon-bearing Agbada Formation. Overlying the prolific Agbada Formation is the Oligocene to Recent Benin Formation which consists of medium to coarse-grained sandstones. The regional lithologic outlook is therefore that of alternating successions of sands and shales (Table.1).
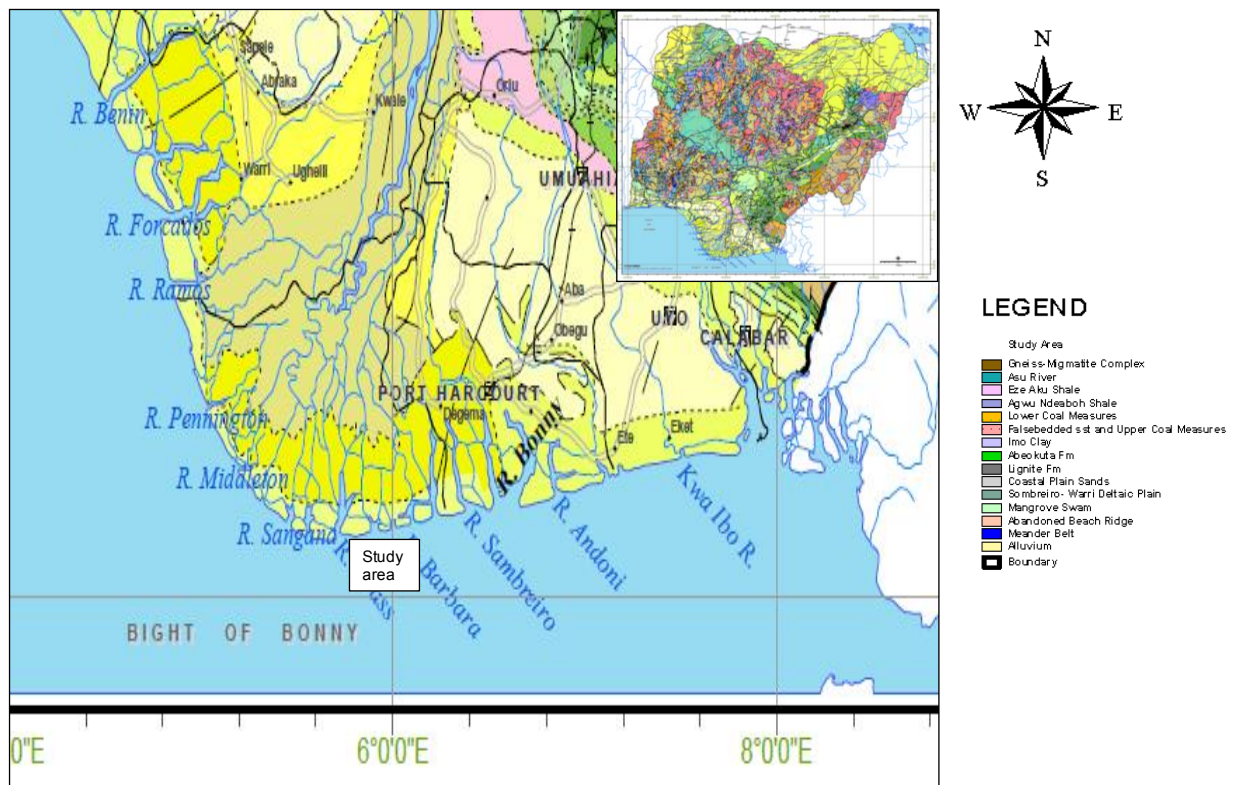


Figure 1 Outline geologic map of Nigeria (inset) showing the study area (source: NGSA, 2006)

Table.1 Main Geologic units of the Niger Delta showing dominant lithology

| Geologic Member | Constituent rock types |
| --- | --- |
| Alluvium | Gravel, sand and argillaceous deposits |
| Freshwater Swamp | Sand, gravel, silt and clay |
| Coastal swamp | Sand (various grains sizes), clay, silt |
| Beach ridges | Sand, clay, silt |
| Deltaic plain | Sand, clay, silt |
| Coastal plain sand (Benin Formation) | Medium to coarse grained sands with clay |
| Agbada Formation | Main reservoir, sand, clay, silt |
| Akata Formation | Major source rock, clay, shale. |

## 3. Materials and Methods

Data used in this study were obtained from a vertical exploration well located in an offshore field in the Niger Delta basin. Available well data were of good quality. These primary data are wireline logs of density, sonic velocity, gamma ray, resistivity and their calculated

derivatives. Sonic, density, and resistivity logs were used to estimate the rock properties within the logged interval of interest as a function of depth. Gamma ray log was basically utilized for lithologic control. The main lithologies distinguished in the gamma ray log are sands and shales using a gamma ray cut of 75 API. Nine (9) RFT pressure measurements were obtained (Table 2) and these were plotted in order to pinpoint normally pressured zones.

Table 2 Measured pore pressure data in the reservoir

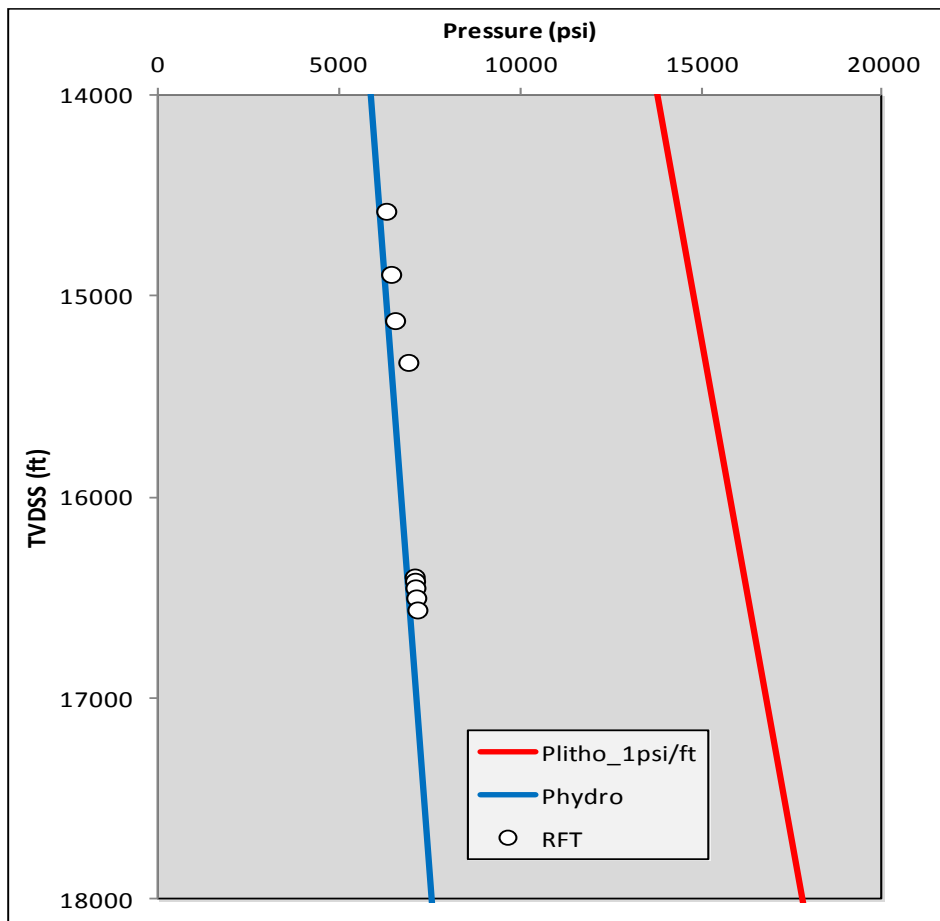| Depth (m) | Depth (ftss) | RFT (psia) | FP gradient (psi/ft) |
|---|---|---|---|
| 4443.9 | 14576 | 6289 | 0.431 |
| 4539.6 | 14890 | 6424 | 0.431 |
| 4609.76 | 15120 | 6533 | 0.432 |
| 4673.17 | 15328 | 6898 | 0.45 |
| 4998.78 | 16396 | 7074 | 0.431 |
| 5005.18 | 16417 | 7084 | 0.432 |
| 5015.24 | 16450 | 7094 | 0.431 |
| 5030.49 | 16500 | 7117 | 0.431 |
| 5048.78 | 16560 | 7148 | 0.432 |



Figure 2 RFT measurements indicate the reservoir is fairly hydrostatic. Data obtained from intervals of rising fluid pressures were excluded from the analysis.

Based on observed pressure magnitudes in Figure 2 above, wireline log data beneath 14100 ft (4300m) were excluded from the study because of the indicated rise in fluid pressures irrespective of the fact that fluid pressure returned to hydrostatic at deeper sections of the well. Such complications in pressure profiles no doubt will affect the final outcome of studies focused on normal fluid pressures that is expected in normally compacted settings. Regression to hydrostatic trends after ramps in fluid pressure often could indicate pressure leakages across incompetent seals.

Trend analyses in this study involved the study of depth variations of elastic properties ($V_p$, $V_s$, and density), acoustic impedances and Poisson's ratio; then cross-plot trends that Vp makes respectively with density and Poisson's ratio in normal pressured zone. The analyses involved observing the relationships between these rock properties with depth and also comparing the trends with established trends in other sedimentary basins of the world.

Well logs obtained after drilling are the most extensively used and reliable means to construct rock models and evaluate formations [3,10,15,17]. For analysis involving formation pressures, Dutta [8] noted that sonic logs are thought to be the best indicators of geopressure because they are relatively less affected by hole size, formation temperature and water salinity. Deviations of sonic transit time away from established normal depth trends are used as indicators of overpressured formations. Data beneath such zones were excluded from the analysis since the interval of interest is the normally pressured. For this work, Ikon Science Software (Rokdoc) was used for easy plotting and calculations.

## 4. Wireline log response of normal pressure formations

Normal pressure formations are able to maintain hydraulic communication with surface during burial such that fluid dissipation continues with increasing sediment load and compaction. Different lithologies compact in different ways. It is therefore necessary to compare similar rock types when dealing with issues of abnormal compaction. Materials like quartz sands suffer elastic compaction under load meaning that the compaction process is largely reversible. Clays suffer plastic deformation that is largely irreversible leading to permanent loss of porosity and permeability. The rate of compaction is governed by the amount and rate of sediment loading and corresponding expulsion of inherent fluids. If rate of sediment loading exceeds that of fluid dissipation, then primary overpressure develops causing changes in rock property trends.
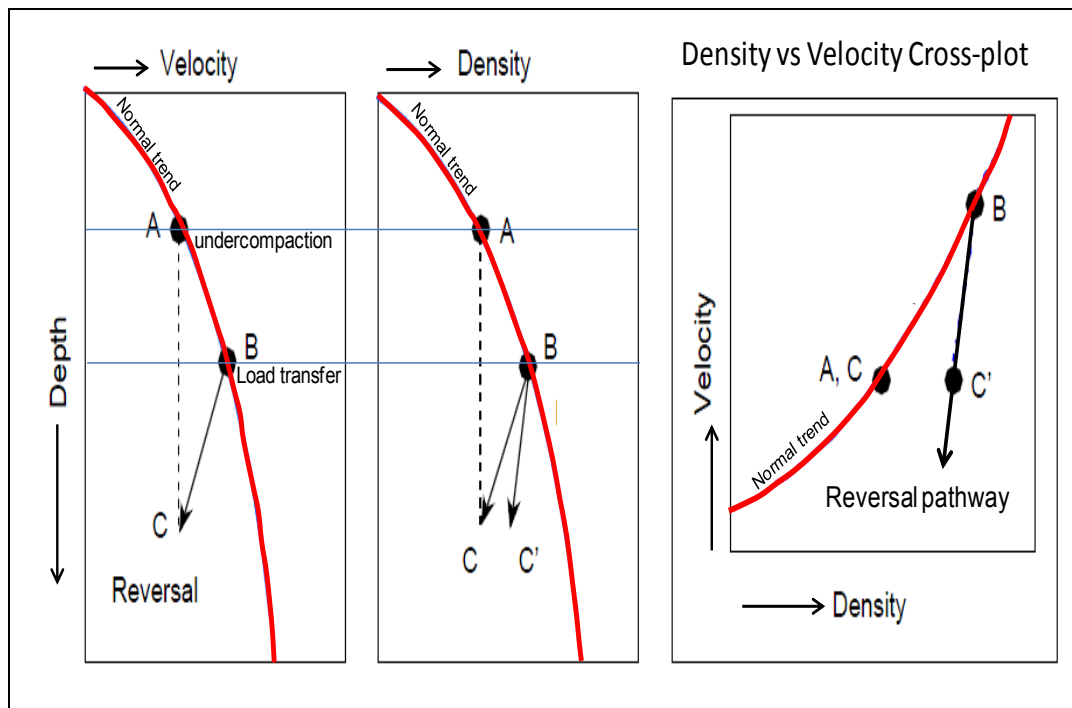


Figure 3 Schematic illustration of trends of velocity and density for shales and resulting cross-plot under different stress regimes (modified from Bowers [4])

Changes in compaction state of rocks can be recognized on regular formation evaluation tools such as sonic, resistivity, porosity, and density logs. These logs show the effects of pore pressure because of the relationship between compaction, porosity, density and the electrical and acoustic properties of sediments. As a rock compacts, the porosity is reduced and the density increases, which also causes the bulk and shear modula to also increase because of increase in grain contact area and stress. Under normal pressure conditions, stress-dependent compaction drives rock properties such as density to the optimal limits

that can be traced out as normal compaction trend or virgin curve (Figure 3). Bowers [4] stresses that density as bulk rock property depends on net pore volume which irreversibly decreases with progressive mechanical compaction. This implies that any factor capable of inducing variations in rock storage pores may leave an imprint on the density log.

For the sonic log, rock properties are controlled by mineral composition and textural characteristics of the rock matrix, volume and interconnection of pore space, nature of contained pore fluids, presence and nature of cementing materials, overburden pressure, internal rock stress as well as burial depth and age of the rock. Sonic velocity logging tools measure the travel time of compressional waves through the rock [16] such that factors that favour internal grain-to-grain contact in the rock matrix cause the sonic logs to trend fastest pathway between the acoustic source and receiver. The normal mechanical compaction of rocks causes an increase in the vertical effective stress (internal rock grain stress) with the result that grain-to-grain contact becomes more effective. Thus, normally compacted intervals are characterized by increase in velocity values as represented by virgin curves or normal compaction trends. With the onset of primary overpressures due to disequilibrium compaction, compaction-driven increase in vertical effective stress becomes greatly retarded such that intergranular contacts is reduced resulting to anomalous porosities. Across this interval of undercompaction, velocity trend slows down substantially causing observable deviation from trend.
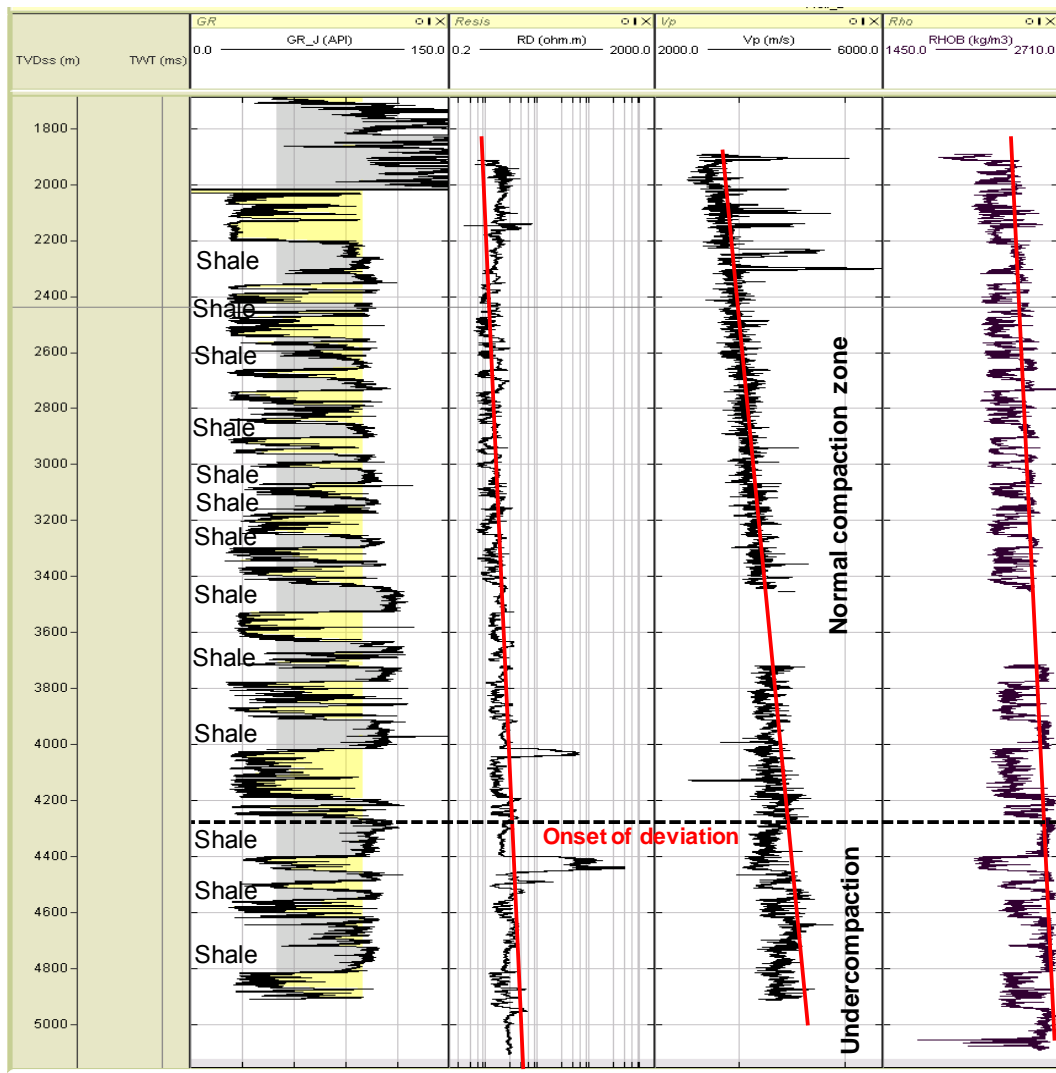


Figure 4 Wireline log data showing rock property depth trends and onset of deviation from normal trend. The deviation from normal trend corresponds with rising fluid pressures at 14100 ft (4300m) in Figure 2 above.

The various porosity-related parameters which are measured as logs can give an insight to the compaction state of the formation when plotted against depth (Figure 4). Their deviations from normal compaction trend could be indicative changes in compaction. Figure 4 shows the wireline log in the study interval. From 2000 m to about 4500 m is an interval characterized by alternating sandstones and shales of various thicknesses. These discrete lithologic units together constitute the reservoir section under study. The mudstone units of interest exceeded 100 ft in thickness and correspond to maximum positive excursions on gamma ray readings (greater than 75 API) that made it easier to distinguish them from silty shales and sandstones.

## 5. Depth trends of velocity (Vp, Vs)

Depth trends of compressional and shear velocities within identified normally pressured intervals of sand and shale have been examined and plotted as Figure 5 and 6 respectively. For both sands and shales, velocities ($V_p$ and $V_s$) tend to bear a linear relationship with depth indicating similar velocity–depth dependence and magnitudes. Smith and Sondergeld [14] also demonstrated that sands and shales have similar velocity-depth dependencies and magnitudes and thus concluded that velocity variations around the best-fit lines could be as a result of many factors such as variations in porosity, shale content, mineralogy, diagenetic overprint, pore pressure, and errors in the logged responses. Oladapo and Adetola [13] observed that at shallower depths, shale velocities are generally higher than those of sands while at greater depths the velocities of sands are higher.
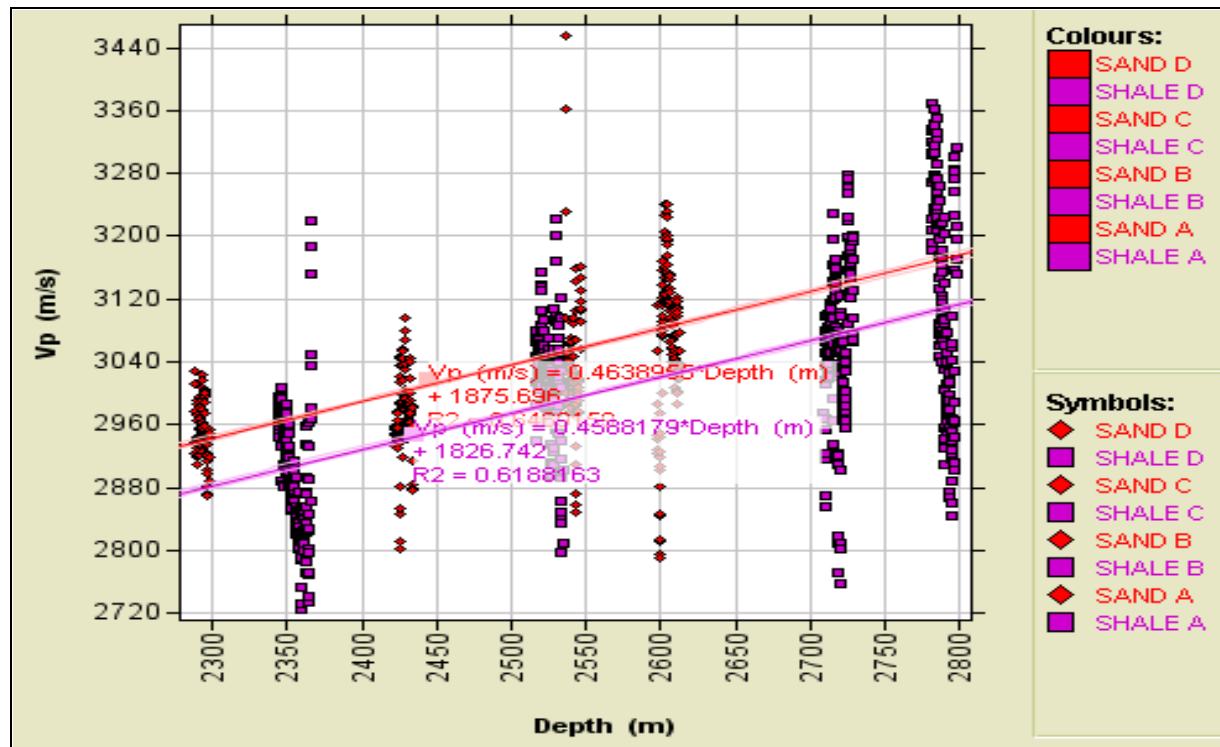


Figure 5 Depth trends of compressional velocity (Vp) for sand and shale with linear regression fits and correlation coefficients Depth-dependent scatter might be a function of limited sampling or alternatively could be ascribed to local variations in porosity, shale content, mineralogy, and diagenetic overprints.

Over the depth ranges of interest, this depth dependence is described by linear trend function for the well. The equations showing the linear relationships between depth (*z* in metres) and *Vp* and *Vs* together with correlation coefficients ($R^2$) generated are as follows:

$$V_p \text{ sand (ms}^{-1}) = 0.4639 \, z \text{ (m)} + 1875.7 \qquad (R^2 = 0.6469) \qquad (1)$$

$$V_p \text{ shale (ms}^{-1}) = 0.4588 \, z \text{ (m)} + 1826.7 \qquad (R^2 = 0.6188) \qquad (2)$$

$$V_s \text{ sand (ms}^{-1}) = 0.4681 \, z \text{ (m)} + 418.0 \qquad (R^2 = 0.7264) \qquad (3)$$

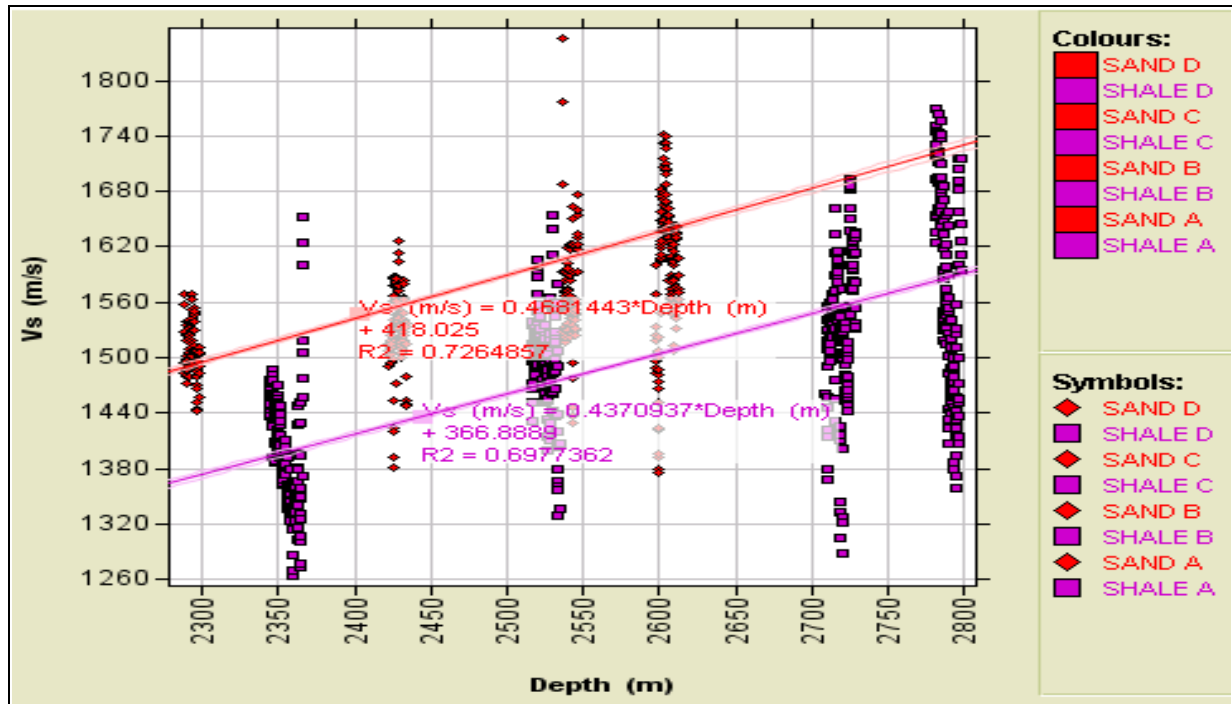$V_s$ shale (ms$^{-1}$) = 0.4371 z (m) + 366.9          ($R^2$ = 0.6977)                    (4)



Figure 6 Depth trends of shear velocity (Vs) for sand and shale with linear regression fits and correlation coefficients

## 6. Depth trends of density ($\rho_b$)

Bulk densities measured on wireline logs were examined with depth. The data shows that for both sands and shales, density trend in normally pressured zone increases linearly with depth as shown in Figure 7.
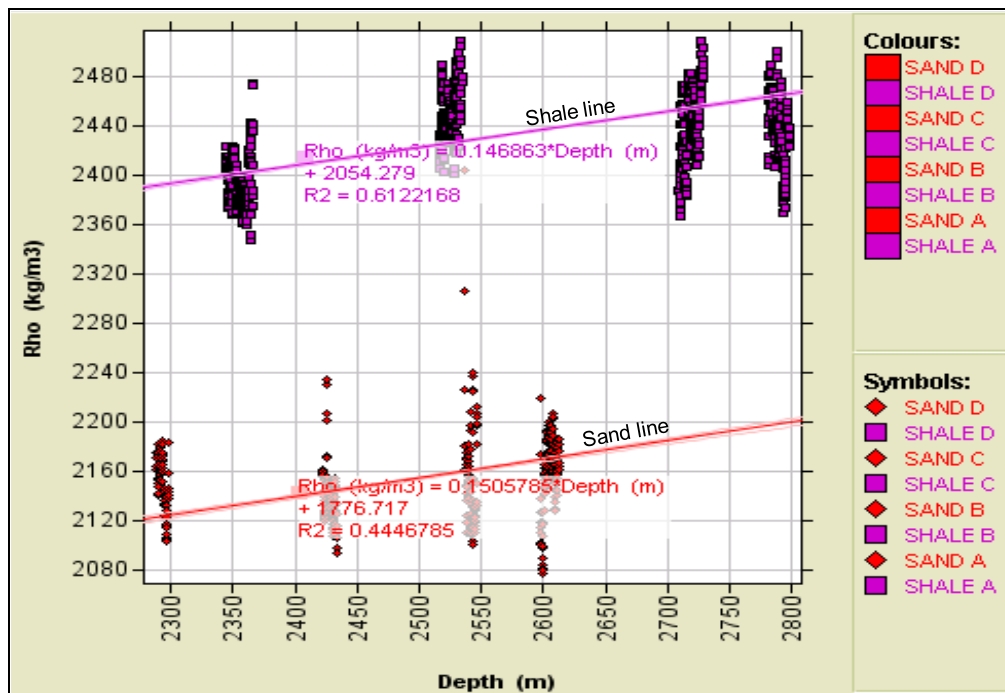


Figure 7 Depth trends of density for both sand and shale. Although densities of both rock types increase linearly with depth, at corresponding depths, shales have higher densities than sand.

A striking observation is that shale densities at corresponding depths are higher than those of sands though both trends are sub-parallel to each other with a gradient difference of 0.0037.

Equations for the linear regression fits show higher values of correlation coefficients for shale. These linear relationships are given below:

$$\rho_b \text{ sand (kgm}^{-3}) = 0.1506\ z\ (m) + 1776.7 \quad (R^2 = 0.4447) \tag{5}$$

$$\rho_b \text{ shale (kgm}^{-3}) = 0.1469\ z\ (m) + 2054.3 \quad (R^2 = 0.6122) \tag{6}$$

## 7. Depth trends of acoustic impedance (AI)

The acoustic impedance (AI) of any material is the product of its density and velocity. It is therefore expected that in normal pressure formations where velocities and densities increase linearly with depth that the acoustic impedance will trend in like manner. A depth plot of acoustic impedance (kgm$^{-2}$ s$^{-1}$) as product of velocity, $V_p$ (m/s) and density (kgm$^{-3}$) for both sands and shales is presented in Figure 8
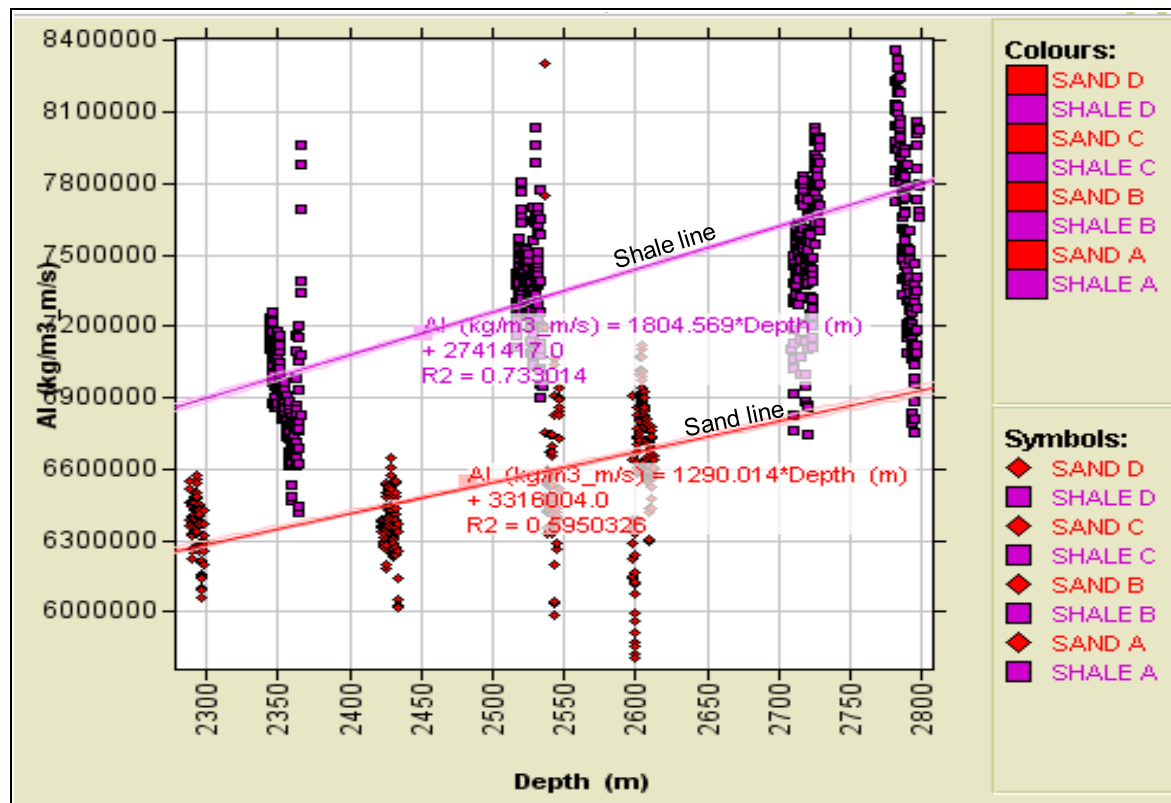


Figure 8 Depth trends of acoustic impedance for sand and shale. Although shales have higher values of AI, divergence between both linear trends tends to increase with depth. Inhomogeneity of the rock types may account for the scatter around the established best fit lines of regression.

The trend indicates that under normal pressure conditions, acoustic impedance increases linearly with depth. Further to this, acoustic impedance values for shales are greater than those for sands with divergence between the two established trends increasing with depth. For instance, a divergence value as much as 100000 kgm$^{-2}$ s$^{-1}$ was observed within a 500 metre interval from 2300 m to 2800 m. This indicates that the sand and shale trends are not parallel to each other but rather on different gradients. The non-homogeneous nature of rock types may be responsible to the long strands of scatter in plotted values. The linear relationships and correlation coefficients generated for sand and shale respectively are given by:

$$\text{AI (kgm}^{-2}\text{ s}^{-1}) = 1290.0\ z\ (m) + 3316004.0 \quad (R^2 = 0.5950) \tag{7}$$

$$\text{AI (kgm}^{-2}\text{ s}^{-1}) = 1804.6\ z\ (m) + 2741417.0 \quad (R^2 = 0.7330) \tag{8}$$

## 8. Depth trends of Poisson's ratio

Poisson's ratio (*v*) is easily determined when Vp and Vs are known. This ratio is important in rock physics calibrations for the discrimination of lithologies. A depth plot of calculated Poisson ratio for both sand and shale is shown as Figure 9.
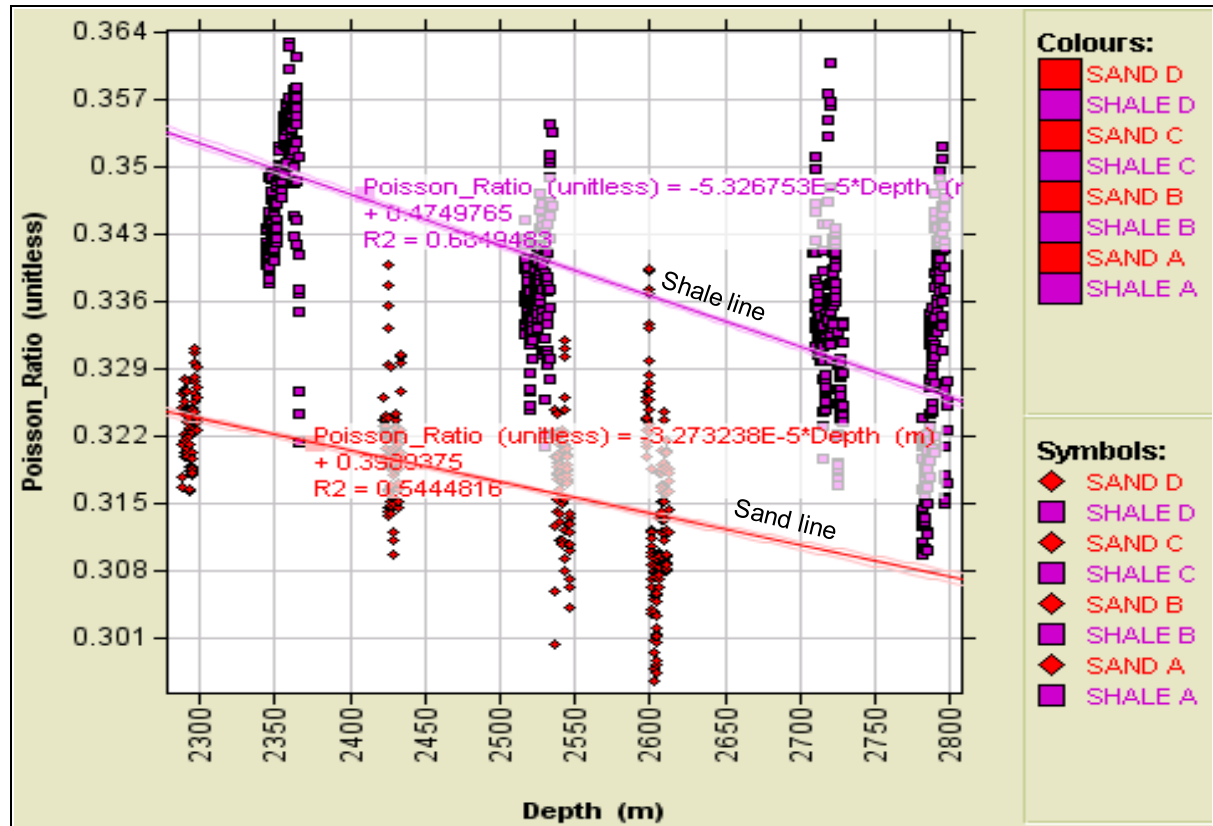


Figure 9 Depth trends of Poisson ratio for both sands and shales in normally compacted zones. A general trend is inversely related to depth

The trend indicates that this parameter decreases with increasing depth of burial in normally compacted settings. Particularly, Poisson's ratios for shales at any target depths are always greater than those of sand. This is in line with laboratory observations of [11]. Correlation coefficients for the linear regression fits are 0.544 and 0.685 for sand and shale lines respectively. The linear trend equations thus generated are given as equations (9) and (10) below:

$$v_{sand} \text{ (unitless)} = -3.2732 \times 10^{-5} z \text{ (m)} + 0.3989 \quad (R^2 = 0.5445) \quad (9)$$

$$v_{shale} \text{ (unitless)} = -5.3268 \times 10^{-5} z \text{ (m)} + 0.4750 \quad (R^2 = 0.6849) \quad (10)$$

## 9. Crossplot trends of density ($\rho_b$) and velocity

Crossplots of density and velocity are good indicators of compaction state of rocks. Density and velocity data presented in previous sections were cross-plotted and examined in order to derive simple empirical trends for the study area. This is shown as Figure 10.

Simple linear trends above indicate that both density and velocity of sands and shales increase with depth in normally pressured formations. This is driven by increase grain to grain contact as result of unrestricted mechanical compaction of the rocks. Shale densities are greater than sand densities with the cross-plot producing a clear line of distinction between both lithologies. The simple linear fit equations and correlation coefficients showing their relationship are derived as follows:

$$\rho_b \text{ (kgm}^{-3}) \text{ sand} = 0.2525 V_p(\text{ms}^{-1}) + 1385.5 \quad (R^2 = 0.5971) \quad (11)$$

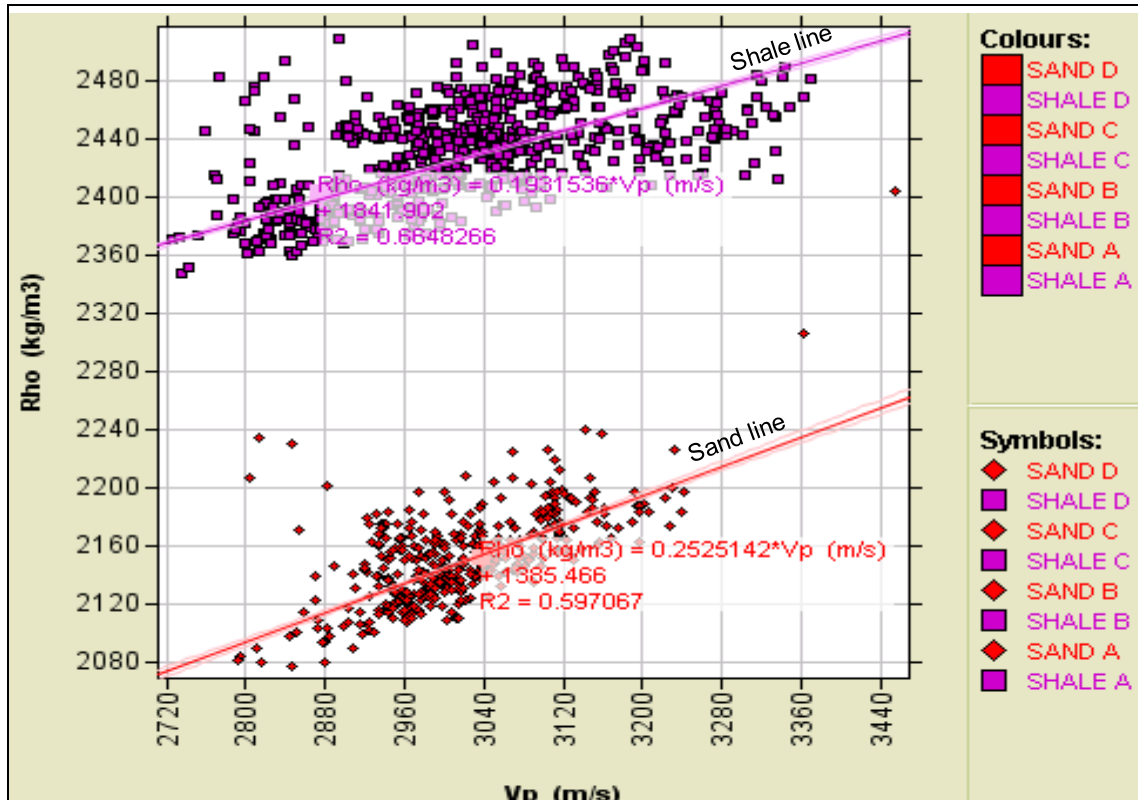$$\rho_b \text{ (kgm}^{-3}) \text{ shale} = 0.1932 V_p(\text{ms}^{-1}) + 1841.9 \quad (R^2 = 0.6648) \quad (12)$$

Figure 10 Cross-plot of density and velocity data for sand and shale

## 10. Cross-plot trends of Poisson's ratio and velocity

Cross-plots of Poisson's ratio and compressional velocities are useful in determining formation characteristics and modeling of physical properties of rocks. Computed Poisson's ratio based on *Vp* and *Vs* values were related with compressional velocity (Figure 11) for both sands and shales.
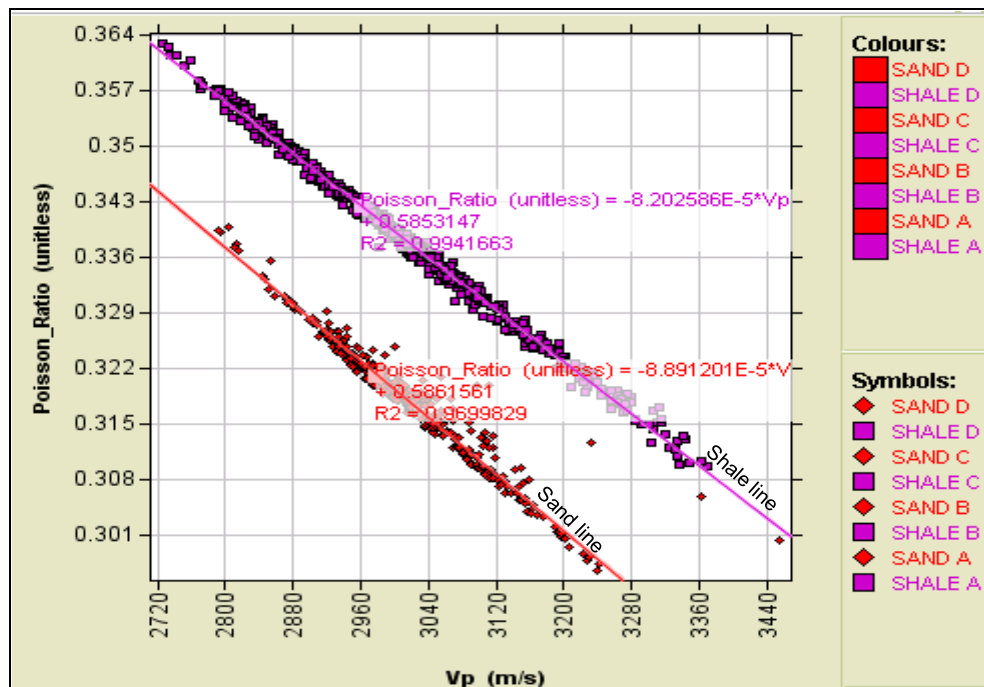


Figure 11 Computed Poisson ratio plotted as a function of velocity for sands and shales with correlation coefficients that approximate to 1.

The plot shows that Poisson's ratio is linearly dependent on velocity; with increasing compressional velocity, Poisson's ratio decreases. Similar linear relationships between Poisson's ratio and $V_p$ for water-saturated rock is documented in Castagna *et al.* [6] who further explained that the high value in shale trend could be largely attributed to clay content. The linear trend equations and better correlation coefficients generated for both sand and shale in the well are given as:

$$v_{sand} \text{ (unitless)} = -8.8912 \times 10^{-5}\, V_p\, (ms^{-1}) + 0.5862 \quad (R^2 = 0.9700) \qquad (13)$$

$$v_{shale} \text{ (unitless)} = -8.2026 \times 10^{-5}\, V_p\, (ms^{-1}) + 0.5853 \quad (R^2 = 0.9942) \qquad (14)$$

## 11. Summary and conclusion

Rock property trends in a normal pressure and normal compacted formation in the Niger Delta largely reflect the inhomogeneous and anisotropic nature of the rocks. Since physical properties of rocks at such zones are dominantly controlled by unimpeded mechanical compaction, it follows that rock properties are at their optimal values with increasing depth. The fourteen linear relationships (equations 1 to 14) developed in this study are derived for sand and shale lithologies using offshore well data in the Niger Delta. Depth trends of compressional velocity ($V_p$), shear velocity ($V_s$), density (ρ) and acoustic impedance (AI) show that these parameters increase with depth while Poisson's ratio (v) trend in the opposite (Figures 6 to 9).

Cross-plots of velocity with density show that both properties progressively increase (Figure 10). A similar plot of velocity and Poisson's ratio shows that both parameters are inversely related (Figure 11). Good correlation coefficients were observed in $V_p$ -depth, $V_s$-depth, Density-depth, acoustic impedance-depth and Poisson's ratio-depth. Poisson's ratio- $V_p$ trends reveal better correlation coefficients. Density- $V_p$ trends generated for shale indicate good correlation coefficients, while sand density- $V_p$ trends indicate poor correlation coefficients. We acknowledge that linear relationships may be an over simplification of the depth trends and cross-plots, the profiles however provide required baseline insights for better constraining and interpretation of seismic data, rock physics models and formation evaluation studies.

## Reference

[1]    Avseth, P., Flesche, H., and Wijngarden, A.V., 2003, AVO classification of lithology and pore fluids constrained by rock physics depth trends. The Leading Edge, vol.22, P. 1004-1011.
[2]    Bachrach, R., Sheila, N., Banik, N., Sengupta, M., Bunge, G., Flack, B., Utech, R., Sayers, C.,Hooyman, P., and Boer, L. D., 2007, From Pore- Pressure prediction to reservoir characterization: A combined Geomechanics-Seismic inversion workflow using trend-kriging  techniques in a deepwater basin, Schlumbergere, Houston, USA. The leading Edge, p. 590-595.
[3]    Bigelow, E. L., 1994, Well logging methods to detection abnormal pressure: In studies in abnormal pressure, ed., Fertl, W. H., Chapman, R. E., and Hotz, R. F., Elsevier.
[4]    Bowers, G. L., 2002, Detecting high overpressure, The Leading Edge, Vol.21, no. 2, p. 174-177.
[5]    Bruce, B., and Bowers, G. L., (2002) Pore pressure terminology. The Leading Edge, Vol.21, No. 2. p. 170-173.
[6]    Castagna, J. P., Batzle, M. l., and Eastwood, R. L., (1985). Relationship between Compressional  - and Shear- waves velocities in elastic Silicate rocks: Geophysics, Vol.50, p. 571-581.

[7]     Chopra, S., and Huffman, A. R., (2006). Velocity determination for pore Pressure predication, Arcis corporarion, Calgary, Alberta, Canada Fusion Petroleum Technologies, Houston, USA.

[8]     Dutta, N., 1987, Geopressure, Geophysics Reprint series, ed., No.7, Society of Exploration Geophysicists, SEG, Tulsa, Ok.

[9]     Gardner, G.H.F., Gardner, L.W., and Gregory, A.R., 1974. Formation Velocity and Density – The Diagnostic basics for Stratigraphic Traps. Geophysics, vol. 39, No. 6, p. 770-780.

[10]    Hottman, C. E., and Johnson, R. K., (1965). Estimation of formation pressures from log derived shale properties. Journal of Petroleum Technol, Vol. 17, p. 717-723.

[11]    Mavko, G., Mukerjii, T., and Dvorkin, J., 1998, The rock physics Hand book: Tools for seismic analysis in porous media. Cambridge University Press.

[12]    Nwozor, K.K., Omudu, M.L., Ozumba, B.M., Egbuachor, C.J., Onwuemesi, A.G., and Anike, O.L., 2013. Quantitative evidence of secondary mechanisms of overpressure generation: insights from parts of Onshore Niger Delta, Nigeria. Petroleum Technology Development Journal, January, 2013 – vol. 1.

[13]    Oladapo, M. I. and Adetola, B. A., (2005). Rock property trend analysis in the Niger Delta Slope. Journal of Geophys. Eng. Vol.2, p.103-110.

[14]    Smith, T. M., and Sondergeld, C. H., (2001). Examination of AVO responses in the eastern deepwater Gulf of Mexico, Geophysics, Vol. 65, p. 1864-1876.

[15]    Timko, D. J., and Fertl, W. H., (1972). How downhole temperatures, pressures affect drilling: prediction hydrocarbon environments with wire line Data: World Oil, Vol. 175 (5).

[16]    Tingay, M.R.P., Hillis, R.R., Swarbrick, R.E., Morley, C.K., 2005. Origin and Petrophysical Log Response of Overpressures in the Baram Delta Province, Brunei. Proceedings, Indonesian Petroleum Association. IPA05-G-093.

[17]    Weakley, R. R., (1989). Recalibration techniques for accurate determination of formation pore pressures from shale resistivity ; SPE Annual Technical Conference and Exhibition, 8-11 October, San Antonio, Texas, http://dx.doi.org/10.2118/19563-MS.